

REPORT DOCUMENTATION PAGE				Form Approved OMB No. 0704-0188	
<p>The public reporting burden for this collection of information is estimated to average 1 hour per response, including the time for reviewing instructions, searching existing data sources, gathering and maintaining the data needed, and completing and reviewing the collection of information. Send comments regarding this burden estimate or any other aspect of this collection of information, including suggestions for reducing the burden, to Department of Defense, Washington Headquarters Services, Directorate for Information Operations and Reports (0704-0188), 1215 Jefferson Davis Highway, Suite 1204, Arlington, VA 22202-4302. Respondents should be aware that notwithstanding any other provision of law, no person shall be subject to any penalty for failing to comply with a collection of information if it does not display a currently valid OMB control number.</p> <p>PLEASE DO NOT RETURN YOUR FORM TO THE ABOVE ADDRESS.</p>					
1. REPORT DATE (DD-MM-YYYY) 20092002		2. REPORT TYPE Proceedings		3. DATES COVERED (From - To)	
4. TITLE AND SUBTITLE SPATIAL AND TEMPORAL VARIABILITY IN BOTTOM ROUGHNESS: IMPLICATIONS TO HIGH FREQUENCY SUBCRITICAL PENETRATION AND BACKSCATTER				5a. CONTRACT NUMBER	
				5b. GRANT NUMBER	
				5c. PROGRAM ELEMENT NUMBER 0601153N	
				5d. PROJECT NUMBER	
6. AUTHOR(S) Kevin L. Williams, Darrell R. Jackson, Eric I. Thorsos, Dajun Tang				5e. TASK NUMBER	
				5f. WORK UNIT NUMBER	
7. PERFORMING ORGANIZATION NAME(S) AND ADDRESS(ES) Naval Research Laboratory Marine Geoacoustics Division Stennis Space Center MS 39529				8. PERFORMING ORGANIZATION REPORT NUMBER NRL/PP/7430-02-4	
9. SPONSORING/MONITORING AGENCY NAME(S) AND ADDRESS(ES) Office of Naval Research 800 North Quincy Street Arlington VA 22217-5000				10. SPONSOR/MONITOR'S ACRONYM(S) ONR	
12. DISTRIBUTION/AVAILABILITY STATEMENT Approved for public release; distribution is unlimited					
13. SUPPLEMENTARY NOTES Impact of littoral environmental variability on acoustic predictions, Lerici Italy, 16-20 Sep 2002					
14. ABSTRACT Quantitative prediction of high frequency, low grazing angle penetration into, and scattering from, sand sediments requires knowledge of the roughness of the water/sand interface. Since the sediment roughness evolves due to hydrodynamic and biological processes, concurrent, co-located measurement of roughness and acoustic penetration/backscattering is essential for testing acoustic models or using such models to determine the likelihood of buried target detection. Here, we examine both roughness and acoustic measurements carried out during a month-long 1999 Sediment Acoustics experiment (SAX99). A ripple field was present throughout the experimental period but changed wavelength and orientation as a result of a storm event (i.e., the ripple field is temporally non-stationary). The predicted impact of this change in the ripple field on acoustic penetration at shallow grazing angles is presented. The small-scale roughness important for backscattering was measured at several locations near to, but not co-located with, acoustic backscattering measurements. These roughness measurements indicate changes with location. The effect of this spatial non-stationarity on tests of alternative backscattering models is discussed. Finally, simple sonar equation predictions of high frequency, low grazing angle buried mine detection are carried out using various combinations of interface roughness conditions.					
15. SUBJECT TERMS sediment interface roughness, sub-critical penetration, backscattering, spatial variability, temporal variability, bottom roughness Sediment Acoustic, SAX99					
16. SECURITY CLASSIFICATION OF:			17. LIMITATION OF ABSTRACT SAR	18. NUMBER OF PAGES 8	19a. NAME OF RESPONSIBLE PERSON Kevin B. Briggs
a. REPORT Unclassified	b. ABSTRACT Unclassified	c. THIS PAGE Unclassified			19b. TELEPHONE NUMBER (Include area code) 228-688-5518

20030220 099

SPATIAL AND TEMPORAL VARIABILITY IN BOTTOM ROUGHNESS: IMPLICATIONS TO HIGH FREQUENCY SUBCRITICAL PENETRATION AND BACKSCATTER.

KEVIN L. WILLIAMS, DARRELL R. JACKSON, ERIC I. THORSOS,
DAJUN TANG

*Applied Physics Laboratory, College of Ocean and Fishery Sciences,
University of Washington, 1013 N.E. 40th St., Seattle, WA 98105 USA
williams@apl.washington.edu*

KEVIN B. BRIGGS

*Marine Geosciences Division, Naval Research Laboratory,
Stennis Space Center, MS 39529 USA
kevin.briggs@nrlssc.navy.mil*

Quantitative prediction of high frequency, low grazing angle penetration into, and scattering from, sand sediments requires knowledge of the roughness of the water/sand interface. Since the sediment roughness evolves due to hydrodynamic and biological processes, concurrent, co-located measurement of roughness and acoustic penetration/backscattering is essential for testing acoustic models or using such models to determine the likelihood of buried target detection. Here, we examine both roughness and acoustic measurements carried out during a month-long 1999 Sediment Acoustics eXperiment (SAX99). A ripple field was present throughout the experimental period but changed wavelength and orientation as a result of a storm event (i.e., the ripple field is temporally non-stationary). The predicted impact of this change in the ripple field on acoustic penetration at shallow grazing angles is presented. The small-scale roughness important for backscattering was measured at several locations near to, but not co-located with, acoustic backscattering measurements. These roughness measurements indicate changes with location. The effect of this spatial non-stationarity on tests of alternative backscattering models is discussed. Finally, simple sonar equation predictions of high frequency, low grazing angle buried mine detection are carried out using various combinations of interface roughness conditions.

1 Introduction

A month-long 1999 Sediment Acoustics eXperiment (SAX99) was carried out to examine scattering from, penetration into, and propagation within a sand sediment at high frequencies [1,2]. One of the goals was to characterize the sediment through out the course of the experiment [2]. The sediment interface roughness was known to be an important factor in at least some aspects of understanding sediment acoustics. Therefore

several means were used to characterize this roughness [2]-[5]. As shown in Section 2, roughness measurements indicate that the sediment interface changes both temporally and spatially.

SAX99 acoustic penetration experiments [6,7] and associated modeling showed that the sediment ripple structure present at the site was the primary sediment feature leading to penetration at grazing angles less than the critical angle (approximately 30°), so called "subcritical" penetration [6]. Other SAX99 experiments quantified the backscattering to an in-water source. Backscatter models [8] were able to predict the scattering levels seen using the sediment roughness measured. However, the spatial changes of measured roughness makes discrimination between models difficult. The effects of temporal and spatial changes in interface roughness on penetration and scattering are presented in Sections 3 and 4.

Detection of a buried target at shallow grazing angles (long ranges) is examined in Section 5 for different sediment ripple wavelengths and rms heights. The signal to noise ratio (SNR) of a buried target is shown to be very sensitive to these two parameters. Also, the spatial variability of the small scale roughness directly effects the uncertainty in the predicted SNR.

2 Sediment Interface roughness

The sand sediment interface roughness at SAX99 was a superposition of a ripple field that can be modeled with a Gaussian spectrum and smaller scale roughness with a power law spectrum. These two components are discussed separately.

2.1 Sand ripples

During SAX99 an autonomous 300 kHz sonar system was fielded that created backscattering images of the sediment interface scattering (see discussion of XBAMS in [1] for details) every 90 minutes from Oct. 6th to Oct. 30th. A storm occurred on Oct 8th that caused a significant change in the ripple field (water depth was about 19 m). Figure 1 shows images of the backscattering (in terms of the Lambert parameter [2]) from the sediment interface generated using scans 36 hrs apart. The ripple field is clearly seen in both images. The storm changes both the wavelength and direction of the ripples. Spectral analysis of the images in Fig. 1 indicate that before the storm the ripple wavelengths were centered on 75 cm while after the storm they were centered on 50 cm.

The storm probably also changed the rms height of the ripple field. No measurements of this height are available for the period before the storm. For the period after the storm (when the majority of SAX99 experiments were carried out) a bottom mounted system, IMP for In situ Measurement of Porosity [2,3], allowed measurement of the rms ripple height as well as the power law portion of the roughness. Figure 2 shows an IMP measurement of a 1 m x 0.15 m section of the sediment interface taken on Oct 18th as well the onedimensional spectrum derived from that measurement. The rms ripple height was approximately 1 cm. Similar results were found using a bottom mounted optical system [5].

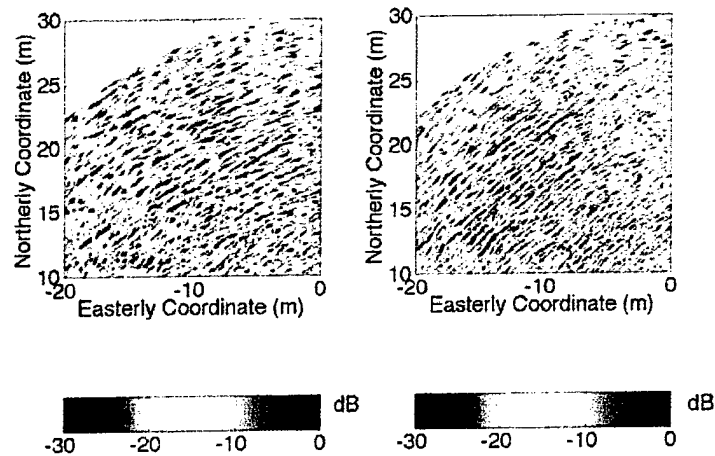


Figure 1. Images of sediment scattering before (left) and after (right) a storm event that caused a change in ripple wavelength and orientation.

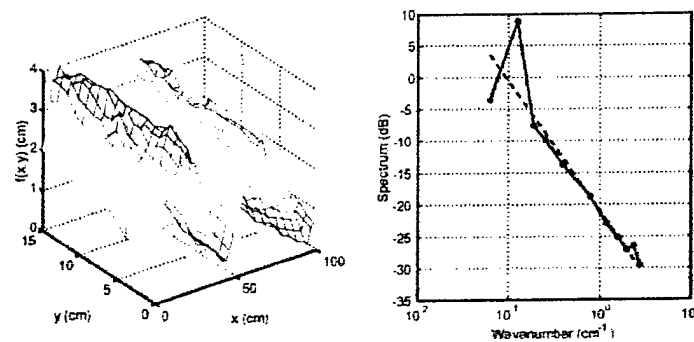


Figure 2. Measurement of a 1m x 0.15 m section of the ripple field present during SAX99 (left). The one dimensional spectrum derived from the measurement (right). The enhanced spectral level at the ripple wavelength is evident.

2.2 Power law interface roughness

Stereo photography measurements [3,4] of the power law portion of the interface roughness were used to examine spatial variability. A two-power law best fit [3] to measured 1-D bottom roughness spectra taken at four different locations within the SAX99 area is shown in Fig. 3 (heavy dashed line segments).

In [3] the roughness profiles from which the spectra were derived were grouped into 4 sets of 3. Each set of 3 profiles was determined from a single stereo pair. The

95% confidence limits associated with each set are presented in [3]. The 95% confidence limits from two of the sets are plotted in Fig. 3. The 95% limits do not overlap over most of the spatial frequency range implying that the roughness at the two locations are not from the same population, i.e., the roughness is spatially nonstationary. This nonstationarity has important ramifications on backscatter model/data comparisons. In particular, estimates of the uncertainty in the spectral level at a site of backscattering measurements must account for this nonstationarity, and these uncertainties need to be used in determining the bounds on model predictions.

For the model/data comparisons of the Section 4 the model uncertainty bounds were estimated by examining the 95% confidence limits in Fig. 3 relative to the best fit line. When plotting model predictions for comparison with data, the model uncertainty was determined by calculating the dB difference between the best fit line and the most extreme upper and lower 95% confidence curve at the spatial frequency appropriate for the acoustic frequency being examined. (Note that Fig. 3 includes vertical dashed lines indicating the spatial frequencies associated with 10° grazing angle backscattering at 20 and 40 kHz.) The uncertainties are for scattering at 20 kHz are +2.4 and -2.7 dB and at 40 kHz are +0.7 and -2 dB.

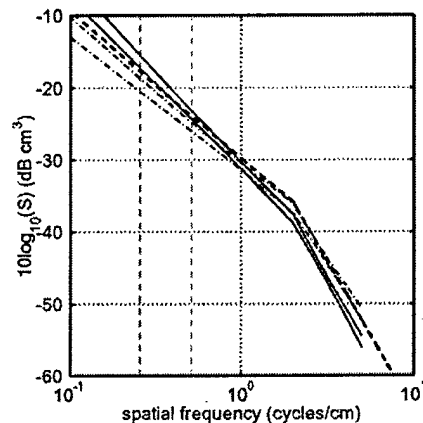


Figure 3. The heavy dashed line segments are best fits to measured bottom roughness spectra taken at four different locations within the SAX99 experimental area. The pairs of solid and dash-dot lines indicate the 95% confidence limits of spectra measured at two locations.

3 Signals received via sub-critical penetration at high frequencies

In [6] a simple diffraction theory model using first order perturbation theory was developed as a starting point to examine subcritical penetration. It was shown that this model captures much of the behavior seen in penetration experiments. Equation 16 of [6] allows calculation of the transmission across the water/sand interface and propagation to a buried target. Reciprocity allows the same expression to handle transmission of the buried target signal back across the interface to an in-water receiver

(to obtain the reciprocal transmission one must multiply the result from Eq. 16 of [6] by the ratio of the water density to the sediment density).

Figure 4 shows the result of a sonar equation calculation for the signal received from a focusing sphere (diameter equal to 25.4 cm) buried such that the top of the sphere is 6.4 cm below the mean water/sand interface. The sand acoustic parameters are given in [6]. The sphere is assumed to have a target strength of -10 dB. A plane wave with a 0 dB re μPa pressure level at the interface is incident at 10° grazing angle with the horizontal component of propagation normal to the ripple strike. The receiver is at a horizontal range of 25 meters and is 4.4 meters above the water/sediment interface (giving a 10° grazing angle as measured from directly above the sphere at the sand/water interface).

The curves in Fig. 4 correspond to the following ripple parameters: 1.ripple wavelength equal 75 cm, ripple rms height equal 1 cm, 2.ripple wavelength equal 50 cm, ripple rms height equal 1 cm, 3.ripple wavelength equal 75 cm, ripple rms height equal 2 cm, 4.ripple wavelength equal 50 cm, ripple rms height equal 2 cm.

From Fig. 4 it is easy to see that if the rms ripple height doubles the received signal for a particular ripple wavelength increases by 12 dB. This is because the transmitted intensity across the water/sand interface (the square of Eq. 16 in [6]) is proportional to the second power of the rms height and the signal must traverse the interface twice to get to the receiver. Also, if one decreases the wavelength from 75 to 50 cm (as occurred because of the storm during SAX99) the peak in the received level for a particular rms ripple height moves to a higher frequency. An explanation for this behavior can be found from the perturbation theory used in the simple diffraction theory of [6]. First order perturbation theory predicts [6] that the angle of transmission into the sediment is given by

$$\cos(\theta_2) = \frac{c_2}{c_1} (\cos(\theta_1) - \frac{\lambda_1}{\lambda_r}) \quad (1)$$

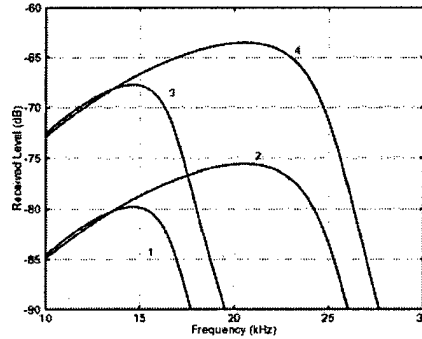


Figure 4. Received pressure levels from a buried sphere for a plane wave incident at a 10° grazing angle onto rippled sand/water interfaces (see text for details).

where c_2 is the sediment sound speed, c_1 is the water sound speed, θ_2 is the transmission grazing angle, θ_1 is the incident grazing angle, λ_1 is the acoustic wavelength

in the water, and λ_r is the wavelength of the ripple. Equation 1 yields a real transmission angle only if the right hand side is less than or equal to 1. This imposes a high frequency cutoff above which the acoustic energy is evanescent (θ_2 becomes complex) and the received level drops rapidly. A smaller λ_r leads to a higher cutoff frequency. This cutoff phenomenon was seen in SAX99 experimental data [6]. The salient point here is that temporal changes in ripple characteristics (wavelength or height) can lead to vastly different buried target receive levels.

4 Testing Backscattering Models

Measured interface roughness was used in [8] to test fluid sediment and Biot sediment backscattering models. Results at 20 and 40 kHz are shown in Fig. 5. The dashed lines in each panel are predictions of the upper and lower bounds for the fluid sediment model and the solid lines are the upper and lower bounds for the Biot model. These bounds were set as discussed in Section 2.2. The asterisks and circles represent data from two different systems [8]. The uncertainty due to the spatial changes in roughness is large enough that it makes discrimination between models difficult. However, data on sound speed dispersion [9] imply that the Biot model is more appropriate for the SAX99 sand. Further modeling [10] has shown that a fluid model of the sediment with an effective density determined from the Biot model gives backscattering results equivalent to the Biot model. In the signal to noise calculations of the next section we have used this effective density.

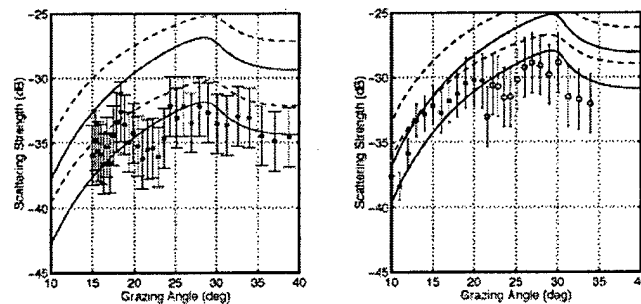


Figure 5. Backscattering from a sand sediment: left-20 kHz, right-40 kHz.

5 High frequency buried target detection at sub-critical angles

The temporal variability of ripple characteristics and spatial variability of the power law roughness have a direct effect on the signal to noise ratios and their uncertainties for buried target detection using high frequency acoustics. The panels in Fig. 6 were calculated using signal levels discussed in Sec. 3 and an ensonified area for backscattering of 0.84 m x 0.3 m. This ensonified area is based on more sophisticated

simulations [6] carried out to determine the region of the sand/water interface that contributes significantly to sub-critical penetration for the geometries of interest.

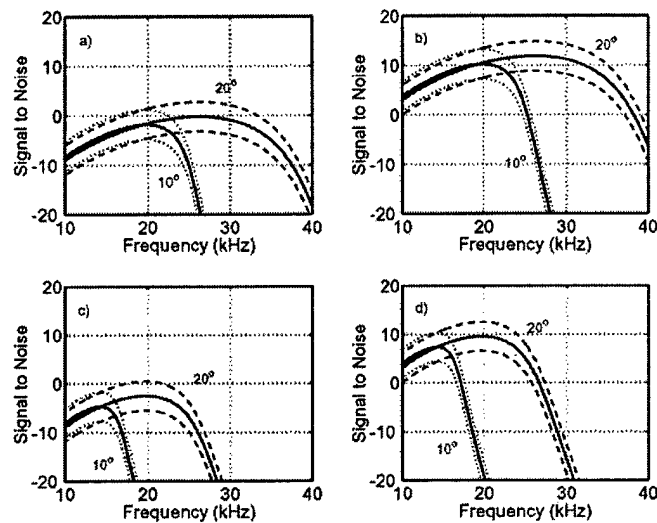


Figure 6. Signal to Noise ratios for a buried target under differing interface conditions and for two different grazing angles. Ripple conditions: a) ripple wavelength (50 cm), rms ripple height (1 cm), b) ripple wavelength (50 cm), rms ripple height (2 cm), c) ripple wavelength (75 cm), rms ripple height (1 cm), d) ripple wavelength (75 cm), rms ripple height (2 cm). The heavy lines in each panel use the mean backscattering level predicted by the Biot model and the lighter lines represent uncertainty bounds based on spatial variability of roughness at scales important for backscattering at 20 kHz.

Comparing panels a and b or c and d demonstrates the sensitivity to ripple height. Likewise, comparing a and c or b and d indicates the importance of ripple wavelength. As an example, for a high resolution sonar (e.g., an Synthetic Aperture Sonar (SAS)) operating at 20 kHz and using a 10° incident angle, the SNR could vary from +10 dB (panel b) to less than -20 dB (panel c) over the conditions used in Fig. 6. Viewed another way, panel b implies that detection of the buried sphere is possible down to 10° when the ripple wavelength is 50 cm but panel d implies detections only down to 20° when the ripple wavelength is 75 cm. Finally, the spatial variability of the power law roughness implies these predicted SNRs have an uncertainty of about ± 3 dB.

From an operational standpoint the sensitivity of detection to roughness conditions implies the need to determine these parameters during mine hunting operations. Obtaining ripple wavelength is easy, indeed SAS images taken during SAX99 allowed ripple wavelength to be determined. Also, the backscattering from the interface is directly obtainable from sonar images if the systems are calibrated. Obtaining ripple rms height is more of a challenge. Current work involves use of backscattering theory and high resolution backscattering images (e.g., Fig. 1) to determine if ripple slopes can be

derived using the backscattered energy from which ripple height could then be determined.

Finally, though the first order perturbation theory used here implies a quick reduction in signal above the cutoff frequency, both experimental evidence and theoretical modeling seem to indicate that higher order effects can be significant contributors to the transmitted signal and allow for continued penetration above the cutoff frequency. Further work is being carried out to investigate these effects.

Acknowledgements

This work was supported by the U.S. Office of Naval Research, Code 3210A.

References

1. Thorsos E. I., et al., "An overview of SAX99: Acoustic measurements," IEEE J. Ocean. Eng., vol. 26, pp. 4-25, 2001.
2. Richardson M. D., et al., "An overview of SAX99: Environmental considerations," IEEE J. Ocean. Eng., vol. 26, pp. 26-54, 2001.
3. Briggs K. B., Tang D. and Williams K. L., "Characterization of interface roughness of rippled sand off Fort Walton Beach, Florida," to be published in IEEE J. Ocean. Eng.
4. Lyons, A. P, Fox W. L. J., Hasiotis T. and Pouliquen E., "Characterization of the two dimensional roughness of wave-rippled sea floors using digital photography," to be published in IEEE J. Ocean. Eng.
5. Moore K. D., and Jules J. S., "Time-evolution of high-resolution topographic measurements of the seafloor using a 3D laser line scan mapping system," to be published in IEEE J. Ocean. Eng.
6. Jackson D. R., Williams K. L., Thorsos E. I. and Kargl S. G., "High-frequency subcritical acoustic penetration into a sandy sediment," to be published in IEEE J. Ocean. Eng.
7. Chotiros, N. P., Smith D. E and Piper J. N., "Refraction and scattering into a sandy ocean sediment in the 30 to 40 kHz band," to be published in IEEE J. Ocean. Eng.
8. Williams K. L., Jackson D. R., Thorsos E. I., Tang D. and Briggs K. B., "Acoustic backscattering experiments in a well characterized sand sediment: Data/model comparisons using sediment fluid and Biot models," to be published in IEEE J. Ocean. Eng.
9. Williams K. L., Jackson D. R., Thorsos E. I. and Tang D., "Comparison of sound speed and attenuation measured in a sandy sediment to predictions based on the Biot theory of porous media," to be published in IEEE J. Ocean. Eng.
10. Williams K. L., "An effective density fluid model for acoustic propagation in sediments derived from Biot theory," J. Acoust. Soc. Am., vol. 110, pp. 2276-2281, 2001.